

## RAPIDITY GAPS AND THE PHOJET MONTE CARLO\*

F.W. Bopp

*Universität Siegen, Fachbereich Physik, D-57068 Siegen, Germany, e-mail: bopp@physik.uni-siegen.de*

R. Engel

*University of Delaware, Bartol Research Institute, Newark, DE 19716 USA, e-mail: eng@lepton.bartol.udel.edu*

J. Ranft

*Universität Siegen, FIGS & Fachbereich Physik, D-57068 Siegen, Germany, e-mail: Johannes.Ranft@cern.ch*

March 1998

A model for the production of large rapidity gaps being implemented in the Monte Carlo event generator PHOJET is discussed. In this model, high-mass diffraction dissociation exhibits properties similar to hadron production in non-diffractive hadronic collisions at high energies. Hard diffraction is described using leading-order QCD matrix elements together with a parton distribution function for the pomeron and pomeron-flux factorization. Since this factorization is imposed on Born graph level only, unitarity corrections lead to a non-factorizing flux function. Rapidity gaps between jets are obtained by soft color reconnection. It was previously shown that this model is able to describe data on diffractive hadron production from the CERN-SPS collider and from the HERA lepton-proton collider. In this work we focus on the model predictions for rapidity gap events in  $p$ - $p$  collisions at  $\sqrt{s} = 1800$  GeV and compare to TEVATRON data.

## I. INTRODUCTION

The PHOJET event generator is a Monte Carlo implementation of the two-component Dual Parton Model. This model combines results obtained within Regge theory, Gribov's reggeon calculus [1,2] and Abramowski-Gribov-Kancheli (AGK) cutting rules [3] with perturbative QCD predictions for hard interaction processes (see for example [4-6], a review is given in [7]).

The Dual Parton Model describes high-mass diffractive hadron production in terms of enhanced graphs like the triple-pomeron graph [8]. As already discussed in [9], within this approach, diffractive processes can be considered as collisions of a color neutral object, the pomeron, with hadrons, photons or other pomerons. However, it is important to note that the pomeron cannot be considered as an ordinary hadron. It is only a theoretical object providing an effective description of the important degrees of freedom of a certain sum of Feynman diagrams in Regge limit (e.g. the available c.m. energy is large compared to the momentum transfer characterizing the scattering process). In this sense, pomeron-hadron or pomeron-pomeron interactions can only be discussed in the framework of collisions of other particles like hadrons or photons.

Experimental data support the interpretation of diffractive particle production in terms of pomeron-hadron or pomeron-pomeron collisions. It was found that high-mass diffraction dissociation exhibits similar features as non-diffractive hadron production where the mass of the diffractively produced system corresponds to the collision energy in non-diffractive interactions [10,11]. Furthermore, it is well known that, in order to obtain a reasonable Monte Carlo description of non-diffractive hadron production, multiple partonic interactions between projectile and target are needed at high energies [12,13,6]. Given the striking similarities between diffractive and non-diffractive multiparticle production one may expect that multiple soft as well as hard interactions may also play an important role in pomeron-hadron/photon/pomeron interactions.

---

\*Talk presented by J. Ranft at LAFEX International School of High Energy Physics, Session C: Workshop on diffractive physics LISHEP98, Rio de Janeiro, Feb.16-20 1998. The PHOJET code and write-up can be obtained from <http://lepton.bartol.udel.edu/~eng/phojet.html>.

Another consequence of the triple-pomeron graph interpretation is an energy-dependent normalization of the pomeron flux. Experimentally, the pomeron flux in target diffraction dissociation is given by the cross section for rapidity gap events divided by the corresponding pomeron-target cross section. However, since at high energies additional projectile-target interactions are likely to fill the rapidity gap with hadrons, the experimentally observable pomeron flux is smaller than the flux implied by the triple-pomeron graph. Furthermore, it may depend not only on projectile but also on target properties.

However, in the case of a large rapidity gap between the jets in two-jet events, as observed at TEVATRON [14,15], at least one pomeron has a large virtuality and standard Regge phenomenology cannot be applied. Therefore, one has to introduce a new kind of process like soft color reconnection (SCR) [16–20] or perturbative gluon-ladder exchange [21,22].

The PHOJET Monte Carlo is a first attempt to build a model which accounts for both effects, multiple soft and hard interactions between the constituents of the projectile and target as well as multiple interactions in the pomeron-projectile, pomeron-target, and pomeron-pomeron scattering subprocesses. The model includes also SCR in hard scattering processes similar to [20].

## II. THE MODEL

The realization of the DPM in PHOJET [23,24] with a hard and a soft component is similar to the event generator DTUJET [6,25] for  $p$ - $p$  and  $\bar{p}$ - $p$  collisions. Interactions of hadrons are described in terms of reggeon ( $\mathbb{R}$ ) and pomeron ( $\mathbb{P}$ ) exchanges. The pomeron exchange is artificially subdivided into *soft* processes and processes with at least one large momentum transfer (*hard* processes). This allows us to use the predictive power of the QCD-improved Parton Model with lowest-order QCD matrix elements [26,27] and parton distribution functions (PDFs). Practically, soft and hard processes are distinguished by applying a transverse momentum cutoff  $p_{\perp}^{\text{cutoff}}$  of about 3 GeV/ $c$  to the scattered partons. The pomeron is considered as a two-component object with the Born graph cross section for pomeron exchange given by the sum of hard and soft cross sections.

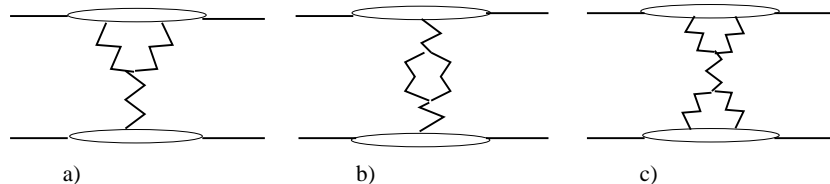


FIG. 1. Enhanced pomeron exchange graphs considered in the model: a) triple-pomeron, b) loop-pomeron, and c) double-pomeron graphs. The zig-zag lines represent pomeron propagators.

High-mass diffraction dissociation is described in the following way. In order to get an efficient parametrization of Born graph cross sections describing diffraction within Gribov's reggeon calculus, we calculate the triple-, loop- and double-pomeron graphs shown in Fig. 1 using a renormalized pomeron intercept  $\alpha_{\mathbb{P}} = 1 + \Delta_{\mathbb{P}} = 1.08$ . The corresponding formulae are given in [28].

Shadowing corrections are approximated by unitarizing the enhanced graphs together with the leading one-pomeron exchange (including soft and hard contributions) in a two-channel eikonal model [6,23,24].

In case of diffractive multiparticle production we have to consider, in addition to the shadowing contribution from multiple pomeron exchange between projectile and target, also rescattering effects in pomeron-hadron and pomeron-pomeron interactions. For the cross section calculation the introduction of a renormalized pomeron trajectory takes this effect into account. However, for the calculation of particle production, a model for the hadronic final states which correspond to the unitarity cut of such a renormalized pomeron propagator is needed. Following Refs. [29,30] we assume that the pomeron-pomeron coupling can be described by the formation of an intermediate hadronic system  $h^*$  the pomerons couple to. Assuming that this intermediate hadronic system has properties similar to a pion, the  $n$ - $m$  pomeron coupling  $g_{n-m}$  reads [30]

$$g_{n-m} = G \prod_{i=1}^{n+m-2} g_{h^* \mathbb{P}} \quad (2.1)$$

with  $g_{h^* \mathbb{P}} = g_{\pi \mathbb{P}}$  being the pomeron-pion coupling.  $G$  is a scheme-dependent constant. Hence, pomeron-hadron and pomeron-pomeron scattering should exhibit features similar to pion-hadron and pion-pion scattering, respectively.

To introduce hard interactions in diffraction dissociation, the impact parameter amplitude of the exchanged (renormalized) pomerons in pomeron–hadron and pomeron–pomeron scattering is again interpreted as the eikonalized amplitude of soft and hard interactions

$$a_{AP}(M_D, \vec{B}) \approx \frac{i}{2} G \left\{ 1 - \exp \left[ -\chi_S^{\text{diff}}(M_D, \vec{B}) - \chi_H^{\text{diff}}(M_D, \vec{B}) \right] \right\} . \quad (2.2)$$

The diffractive eikonal functions read

$$\chi_S^{\text{diff}}(M_D, \vec{B}) = \frac{g_{AP}^0 g_{h^*P}^0 (M_D^2/s_0)^{\Delta_P}}{8\pi b_P(M_D^2)} \exp \left( -\frac{\vec{B}^2}{4b_P(M_D^2)} \right) \quad (2.3)$$

$$\chi_H^{\text{diff}}(M_D, \vec{B}) = \frac{\sigma_{\text{hard}}^{AP}(M_D^2)}{8\pi b_{h,\text{diff}}} \exp \left( -\frac{\vec{B}^2}{4b_{h,\text{diff}}} \right) , \quad (2.4)$$

where  $\sigma_{\text{hard}}^{AP}$  is the parton model cross section for hard pomeron– $A$  scattering ( $A$  can be a hadron, photon or pomeron). In all calculations the pomeron PDFs proposed by Capella, Kaidalov, Merino, and Tran (CKMT) [31,32] with a hard gluon component are used.

To estimate the sensitivity of the model results to non-factorizing coherent pomeron contributions as proposed in [33,34], we use optionally also a toy model with a direct pomeron–quark coupling [35]. In this case, the pomeron is treated similar to a photon having a flavor independent, unknown quark coupling  $\lambda$ . The corresponding matrix elements are given in [36].

### III. SOFT COLOR RECONNECTION

Both the CDF and D0 collaborations have found dijet production by color–singlet exchange [14,15]. These Jet–gap–Jet (JgJ) events are not due to traditional diffractive processes. The two jets separated by a rapidity gap are in polar angle back–to–back correlated. Certainly in double–diffractive events describing the diffractively produced systems on both sides of the gap by pomeron–hadron scattering, we would also find jets, but these jets would not be back–to–back correlated. Therefore, we have to consider these events as mainly due to a new mechanism of hard pomeron exchange.

To describe these events within the PHOJET Monte Carlo, we introduce SCR between hard scattered partons in nondiffractive events following Eboli, Gregores and Halzen [20]. This mechanism is quite similar to the the soft color interaction mechanism described by Ingelman [37]. We use the following SCR probabilities [20] in PHOJET

$$F_{qq} : F_{qg} : F_{gg} = \frac{1}{9} : \frac{1}{24} : \frac{1}{64} . \quad (3.1)$$

The simplest hard q–q event, where SCR leads to a rapidity gap between two jets is an event with just one single hard valence–quark – valence–quark scattering. In normal events in the Dual Parton Model we get two color strings each being stretched between one scattered quark and the diquark of the other hadron, no rapidity gap is present in such events. In events with SCR we get a color reconnection caused by the exchange of soft gluons, now the color strings connect the hard scattered quark and the diquark of the same hadron, these are events with a rapidity gap.

The simplest hard g–g event where SCR leads to a rapidity gap between two jets is an event with just one hard g–g scattering. In normal events we get again two color strings connecting the (soft) valence quark of one hadron via the hard scattered gluon to the (soft) diquark of the other hadron. In events with SCR the color strings are stretched from the (soft) valence quark of one hadron via one hard scattered gluon to the (soft) diquark of the same hadron. Such events might have a rapidity gap.

In most events we have multiple soft and hard interactions, even if a rapidity gap appears in one of the multiple collisions, the gap might be filled by hadrons resulting from the other collisions. The Monte Carlo simulation of complete events incorporates this effect, in this way PHOJET accounts already for the gap survival probability [38,39].

### IV. PREVIOUS COMPARISONS WITH HADRON–HADRON AND PHOTON–HADRON DATA

## A. Diffractive cross sections

Studying diffractive cross sections is not the primary concern of this paper. Results on diffractive cross sections were already presented using the DTUJET model in Refs. [6,40,25] and using the present PHOJET model in Refs. [23,28], we include updated results for these cross sections here.

In Fig. 2.a data on single diffractive cross sections [41–49] are compared with our model results ( $M_D^2 < 0.05s$ ). It is to be noted that the data on single diffractive cross sections at collider energies are subject to large uncertainties. Nevertheless the rise of the cross section from ISR energies to the energies of the CERN and FERMILAB colliders is less steep than expected from the Born level expression which is the triple pomeron formula. However, within our model a renormalized pomeron flux as proposed in [50] is not needed. There are two reasons this:

(i) The eikonal unitarization procedure in the model suppresses the rapidity gap survival probability. This effect is well known (see for example [51,52]) and can be tested directly comparing diffraction dissociation in deep inelastic scattering and photoproduction at HERA [39].

(ii) The graph for double-pomeron scattering has cuts which correspond to single diffraction dissociation. However, due to the negative sign of these contributions the diffractive cross section is significantly reduced at high energies as compared to a model with an eikonalized triple pomeron graph only [53].

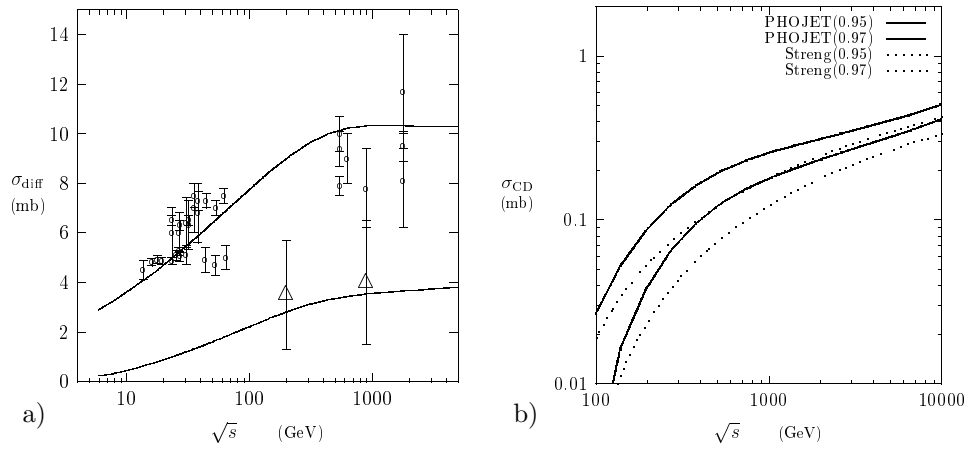


FIG. 2. (a) Single and double diffractive  $p - \bar{p}$  cross sections as a function of the center of mass energy  $\sqrt{s}$ . Model results are compared to data on single diffractive cross sections [41–49]. In addition, some experimental estimates for the cross section on double diffraction dissociation [45,46] are shown (triangles). (b) The energy dependence of the central diffraction cross section. We compare the cross section as obtained from PHOJET with unitarization using a supercritical pomeron with the cross section obtained by Streg [54] without unitarization and with a critical pomeron. Both cross sections are for the same two kinematic cuts:  $M_{\text{CD}} > 2 \text{ GeV}/c^2$  and Feynman- $x$  of the scattered hadron  $x_F > 0.95$  (upper curves) and 0.97 (lower curves).

In Fig. 2.b we compare as function of the energy the central diffraction cross sections in proton-proton collisions, which we obtain from PHOJET with the cross section calculated by Streg [54]. In PHOJET we use a supercritical pomeron with  $\Delta_{\bar{P}} = 0.08$  whereas Streg [54] uses a critical Pomeron with  $\Delta_P = 0$ . Note that also the double-pomeron cross section grows in Born approximation with  $s$  like  $\sim s^{2\Delta_{\bar{P}}}$ . This rapid increase is damped in PHOJET by the unitarization procedure. At high energies, contributions from multiple interactions become important. The rapidity gaps are filled with hadrons due to inelastic rescattering and the cross section for central diffraction gets strongly reduced. In contrast, Streg calculates only the Born term cross section. Figure 2.b illustrates the differences obtained using different theoretical methods. We stress, both methods use the measured single diffractive cross sections to extract the triple-pomeron coupling.

## B. Diffractive hadron- and jetproduction

There are some experiments on diffractive particle production at colliders, which we have studied previously using PHOJET [36,55]. Generally, we have reached a good agreement. We do not present these comparisons again here.

Among others, the following experiments have studied hadron production in single diffraction dissociation at the CERN-SPS and DESY-HERA and colliders:

1. The UA-4 Collaboration [56,11,57] measured pseudorapidity distributions of charged hadron production for different masses of the diffractive system. We have already twice compared earlier versions of the Dual Parton Model [58,59] to this data. New in the present model is hard diffraction and multiple interactions in the diffractive hadron production, therefore we have again compared to this data and we find a reasonable agreement [36]. In the model, multiple interactions and minijets lead to a rising rapidity plateau in pomeron-proton collisions in a similar way as observed in hadron-hadron collisions.
2. Hard diffractive proton-antiproton interactions were investigated by the UA-8 Collaboration [60]. In this experiment the existence of a hard component of diffraction was demonstrated for the first time. Because of the importance of these findings, we compared them already in [55] to our model and found the model to be consistent with this experiment. Therefore we will not repeat this comparison here.
3. Results on single photon diffraction dissociation and in particular hard single diffraction were presented by both experiments at the HERA electron-proton collider [61-65]. The ZEUS Collaboration [64] has presented differential and integrated jet pseudorapidity cross sections for jets with  $E_{\perp}^{\text{jet}} > 8$  GeV. The absolute normalization of these data is given. This allows a severe check of the model. In [36] we have compared the differential jet pseudorapidity cross sections from ZEUS [64] to the model.

## V. COMPARING HADRON PRODUCTION IN DIFFRACTIVE PROCESSES TO NON-DIFFRACTIVE PARTICLE PRODUCTION IN $P$ - $P$ AND $\gamma$ - $\gamma$ REACTIONS

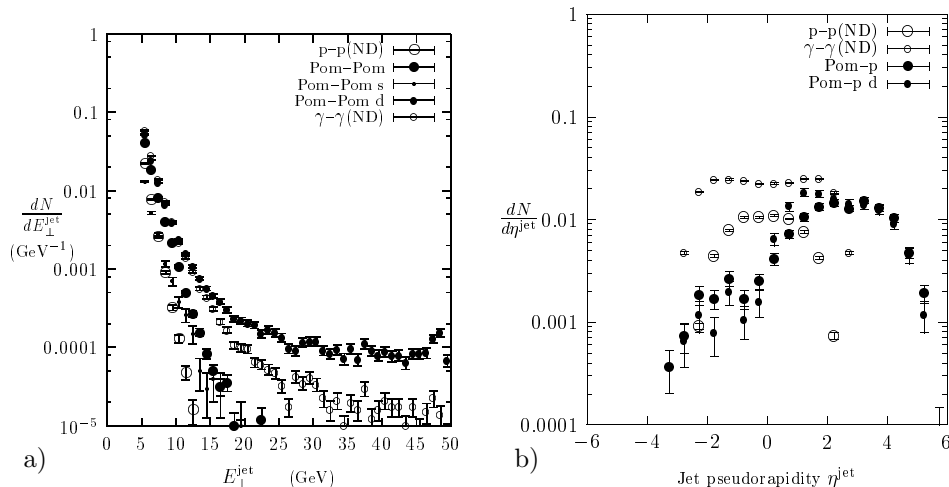


FIG. 3. (a) Jet transverse energy distributions in non-diffractive  $p$ - $p$  and  $\gamma$ - $\gamma$  collisions compared with the jet transverse energy distribution in central diffraction (pomeron-pomeron collisions). For the latter channel we give the distributions separately for the full model, the model without multiple interactions (s) and the model with a direct pomeron coupling (d). The distributions were generated with PHOJET, the c.m. energy / diffractive mass is 100 GeV in all cases. (b) Jet pseudorapidity distributions in non-diffractive  $p$ - $p$  and  $\gamma$ - $\gamma$  collisions compared with the jet pseudorapidity distribution in single diffraction (pomeron- $p$  scattering). The distributions were generated with PHOJET, again the c.m. energy / diffractive mass is 100 GeV in all cases, but the pseudorapidities in the collisions with pomerons given refer to the  $\sqrt{s} = 2$  TeV  $p$ - $p$  collisions used to generate the diffractive events.

In Sections II we have already pointed out, that our model for particle production in pomeron-hadron/photon collisions and pomeron-pomeron collisions has the same structure characterized by multiple soft collisions and multiple minijets like models for hadron production in non-diffractive hadron-hadron collisions. Therefore, again we expect the main differences in comparison to other channels in the hard component due to the differences between the pomeron and hadron structure functions and due to the existence or nonexistence of a direct pomeron-quark coupling.

The differences in the parton structure functions of protons, photons and pomerons lead to quite different energy dependences of the hard cross sections. In all processes where pomerons are involved, single diffraction and central diffraction, hard processes become important already at lower energies. For pomeron-pomeron scattering at low energy the hard cross section is about a factor 100 bigger than that of  $p$ - $\bar{p}$  collisions. At high energies the opposite happens, the hard cross sections in all processes where pomerons are involved rise less steeply with the energy than in purely hadronic or photonic processes. The reason for this is the different low- $x$  behavior of the parametrization

of the structure functions used. However, nothing is known at present from experiment about the low- $x$  behavior of the pomeron structure function.

In Fig. 3.a we compare jet transverse energy distributions in  $p$ - $p$  and  $\gamma$ - $\gamma$  collisions with the ones in  $\mathbb{P}$ - $\mathbb{P}$  collisions. In the channels with pomerons we present again the distributions according to our full model, according to the model without multiple interactions and the model with a direct pomeron-quark coupling. In all non-diffractive collisions we have  $\sqrt{s} = 100$  GeV and the diffractive events are generated in  $\sqrt{s} = 2$  TeV collisions with  $M_D = 100$  GeV/ $c^2$ . The differences in the jet transverse energy distributions between the channels are as to be expected more pronounced than in the hadron  $p_\perp$  distributions. We observe an important reduction in the jet distributions in the model without multiple interactions. The effect of the direct pomeron coupling is as dramatic as the effect due to the direct photon coupling. The  $E_\perp$  distributions in the  $\mathbb{P}$ - $\gamma$  and  $\mathbb{P}$ - $\mathbb{P}$  channels extend up to the kinematic boundary. In the latter two cases as in the case of  $\gamma$ - $\gamma$  collisions the entries at large  $E_\perp$  come only from direct processes.

In Fig. 3.b we compare jet pseudorapidity distributions in  $p$ - $p$ ,  $\gamma$ - $\gamma$  and  $\mathbb{P}$ - $p$ , again, all collisions at  $\sqrt{s} = 100$  GeV with the diffractive events generated in  $\sqrt{s} = 2$  TeV collisions. For the jets we observe substantial differences in the shape of the pseudorapidity distributions.

## VI. SINGLE DIFFRACTION AND CENTRAL DIFFRACTION AT TEVATRON

In Figs. 4 to 5.b we present some cross sections calculated using PHOJET at TEVATRON energy. The distributions are mass distributions in single and central diffraction (Fig. 4) and jet pseudorapidity distributions in single and central diffraction using  $E_\perp$  thresholds of 5 and 15 GeV (Fig. 5.a and .b). In all Figs. we give the plots for three different cuts for the Feynman- $x$  of the diffractive nucleons  $x_F > 0.9$ , 0.95 and 0.97. It is obvious, that all distributions and cross sections depend strongly on these cuts.

One of the results obtained by the D0 Collaboration is the ratio of double-pomeron exchange (DPE)<sup>1</sup> to non-diffractive (ND) dijet events [66]:

$$\left( \frac{\sigma(\text{DPE})}{\sigma(\text{ND})} \right)_{E_\perp^{\text{jct}} > 15 \text{ GeV}} \approx 10^{-6} \quad (6.1)$$

Within the PHOJET model one gets the following cross sections:

Non-diffractive interactions (ND):  $\sigma(\text{ND}) = 45.2$  mb,

Both-side single diffraction dissociation (SD):  $\sigma(\text{SD}) = 11.2$  mb,

Central diffraction (CD):  $\sigma(\text{CD}) = 0.64$  mb.

From these cross sections together with Figs. like 5 we get, always calculated for  $E_\perp^{\text{jct}}$  larger than 15 GeV:

$$(\text{CD})/(\text{ND}) \approx 2 \times 10^{-6},$$

$$(\text{SD})/(\text{ND}) \approx 4 \times 10^{-3},$$

$$(\text{CD})/(\text{SD}) \approx 0.5 \times 10^{-3}.$$

Despite the fact that no experimental acceptance has been considered for these PHOJET results it is interesting to find the (CD)/(ND) ratio so close to the D0 value given above.

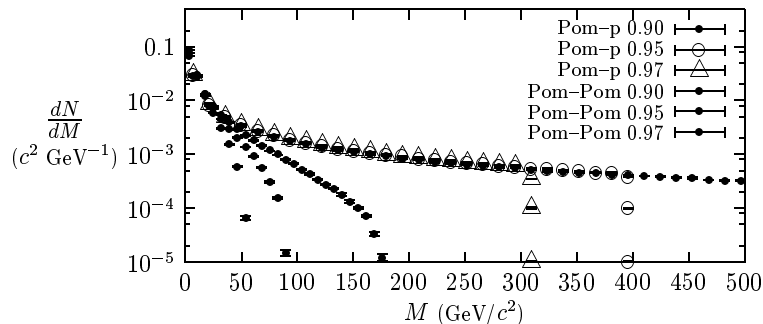


FIG. 4. Distribution of the diffractive mass in single diffraction dissociation (pomeron-proton) and central diffraction (pomeron-pomeron) at TEVATRON with  $\sqrt{s} = 1.8$  TeV for three different cuts of the Feynman- $x$  of the diffractive nucleons.

<sup>1</sup> In [66] the term double-pomeron exchange is used instead of central diffraction.

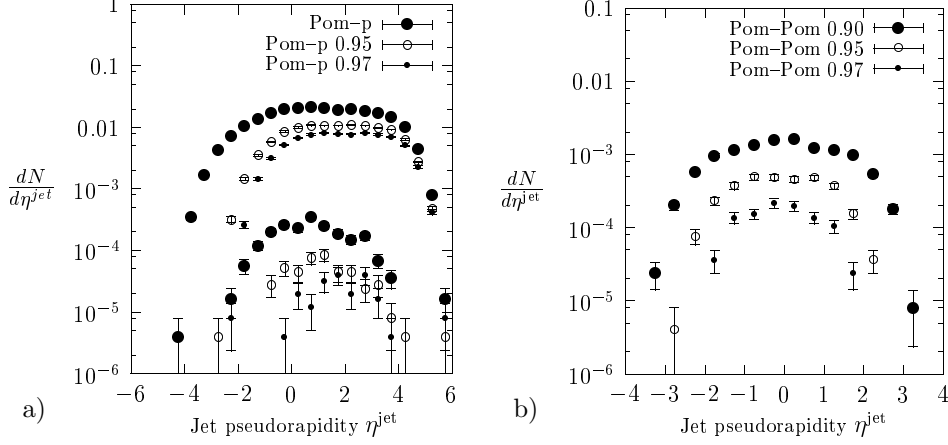


FIG. 5. (a) Pseudorapidity distribution of jets with  $E_{\perp}$  larger than 5 GeV and 15 GeV in (one side) single diffraction (Pom-p) at TEVATRON for three different cuts of the Feynman- $x$  of the diffractive nucleon. The upper curves with the same plotting symbol are generally for  $E_{\perp} = 5$  GeV, the lower curves are for  $E_{\perp} = 15$  GeV. (b) Pseudorapidity distribution of jets with  $E_{\perp}$  larger than 5 GeV in central diffraction (Pom-Pom) at TEVATRON for three different cuts of the Feynman- $x$  of the diffractive nucleons.

## VII. DIFFRACTIVE DIJET PRODUCTION AT TEVATRON

Data on dijet production in single diffraction dissociation using a rapidity gap trigger were published by the CDF Collaboration [67]. Same side ( $\eta^{\text{jet}1} \times \eta^{\text{jet}2} > 0$ ) dijets were selected with  $E_{\perp}^{\text{jet}} > 20$  GeV in the jet pseudorapidity window  $1.8 < |\eta^{\text{jet}}| < 3.5$ . The gap trigger did demand no charged hadrons in the range  $3.2 < |\eta| < 5.9$  opposite to the jets and no calorimeter hit above 1.5 GeV in the range  $2.4 < |\eta| < 4.2$  opposite to the jets. The ratio of dijet events with gap (JJg) to dijets without gap (JJ) was found to be

$$R_{\text{JJg-CDF}} = \frac{(\text{JJg})}{(\text{JJ})} = (0.75 \pm 0.05 \pm 0.09)\% . \quad (7.1)$$

Using PHOJET we got so far good statistics only for  $E_{\perp}^{\text{jet}} > 10$  GeV when using the CDF pseudorapidity restrictions. We obtained the cross sections  $\sigma_{\text{JJ}} = 50.4 \mu\text{b}$  and  $\sigma_{\text{JJg}} = 0.107 \mu\text{b}$ . This gives the ratio  $R_{\text{JJg-PHOJET}} = 0.21\%$ . There are two possible reasons for this ratio being smaller than the one found by CDF: (i) the different  $E_{\perp}$  cut and (ii) The CKMT pomeron structure functions [31,32] used in the calculation might not contain enough hard gluons.

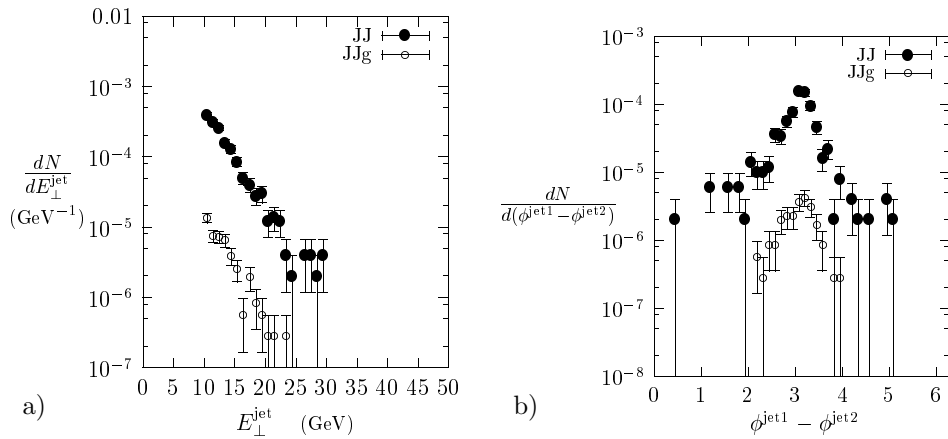


FIG. 6. (a)  $E_{\perp}^{\text{jet}}$  distributions in JJ and JJg events obtained in PHOJET using the CDF triggers. (b)  $\phi^{\text{jet}1} - \phi^{\text{jet}2}$  distributions in JJ and JJg events obtained with PHOJET using the CDF trigger.

In Fig.6.a we present  $E_{\perp}^{\text{jet}}$  distributions calculated from PHOJET for the JJ and JgJ events. Within the statistics of the Monte Carlo calculation both distributions seem to have the same shape.

In Fig.6.b we present  $\phi^{\text{jet1}} - \phi^{\text{jet2}}$  distributions for the JJ and JgJ events. Again within the statistics both distributions seem to be quite similar. However, in the JJ events we find more often additional jet-pairs than in the JgJ events. Therefore we would expect a more narrow correlation of the two jets in the JgJ events.

### VIII. DIJET PRODUCTION BY COLOR-SINGLET EXCHANGE AT TEVATRON

We will refer here only to the data on dijet production by color-singlet exchange published by the CDF and D0 Collaborations [14,15]. More preliminary data have been presented at this meeting.

D0 [14] finds opposite side ( $\eta^{\text{jet1}} \times \eta^{\text{jet2}} < 0$ ) dijets with  $E_{\perp}^{\text{jet}} > 30$  GeV and  $|\eta^{\text{jet}}| > 2$ . The pseudorapidity gap is at  $|\eta| < 1.3$ . The fraction of JgJ events is found to be

$$R_{\text{JgJ-D0}} = \frac{(\text{JgJ})}{(\text{JJ})} = (1.07 \pm 0.10^{+0.25}_{-0.13})\% \quad (8.1)$$

CDF [15] uses opposite side jets with  $E_{\perp}^{\text{jet}} > 20$  GeV and  $3.5 > |\eta^{\text{jet}}| > 1.8$  with a gap at  $|\eta| < 1.0$ . The gap fraction is found to be

$$R_{\text{JgJ-CDF}} = \frac{(\text{JgJ})}{(\text{JJ})} = (1.13 \pm 0.12 \pm 0.11)\% . \quad (8.2)$$

Furthermore, the jets are found to be back-to-back correlated in  $\phi^{\text{jet1}} - \phi^{\text{jet2}}$ .

In PHOJET using SCR model as described in Section III we find with the D0 trigger

$$R_{\text{JgJ-PHOJET-D0}} = \frac{(\text{JgJ})}{(\text{JJ})} = 0.43\% . \quad (8.3)$$

Here 0.1% background JgJ events with only an accidental gap was subtracted, this background was determined in a run without the use of SCR.

With the CDF trigger we find

$$R_{\text{JgJ-PHOJET-CDF}} = \frac{(\text{JgJ})}{(\text{JJ})} = 0.50\% \quad (8.4)$$

where 0.5% background JgJ events had to be subtracted.

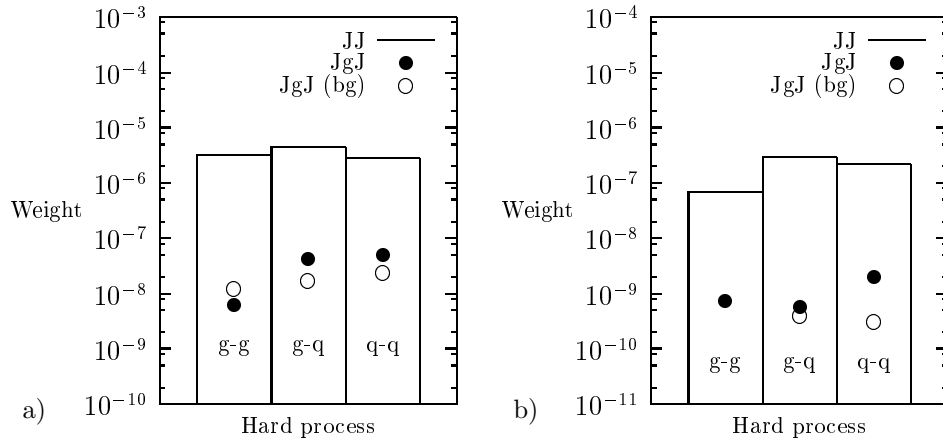


FIG. 7. (a) Monte Carlo predictions for the fractions of g-g, g-q and q-q hard scatterings in the JJ events (without gap trigger), JgJ events obtained with SCR and background (bg) JgJ events (obtained without SCR) for the CDF trigger. (b) The fractions of g-g, g-q and q-q events for JJ events (without gap trigger), JgJ events obtained with SCR and background (bg) JgJ events (obtained without SCR) for the D0 trigger.

In the PHOJET Monte Carlo we can subdivide the hard scattering events into g-g, g-q and q-q scatterings. In Fig.7 we plot for the CDF and D0 triggers the fractions of g-g, g-q and q-q events for JJ events (without gap trigger), JgJ events obtained with SCR and background JgJ events (obtained without SCR). At both energies we find, that q-q scattering dominates the JgJ events, but g-q and g-g scattering contributes also. For the q-q events the fraction of JgJ events due to SCR (background subtracted) is always smaller than 1% of the q-q scatterings without gap. In principle we could calculate from this separately the gap survival probabilities for q-q, g-q and g-g scatterings, with the present statistics of JgJ events however, we prefer not yet to give such numbers. In JgJ events we find generally only one or two pairs of jets whereas in events without a large gap the average number of jets is definitely larger than this.

In Fig. 8.a we present the  $\phi^{\text{jet1}} - \phi^{\text{jet2}}$  distribution calculated with PHOJET for the JJ and JgJ events for the CDF trigger together with the corresponding distribution published by CDF [15]. All distributions are rather similar. However, with bigger statistics we expect to see a more narrow correlation in the JgJ events, in which further jets are much less frequent than in the JJ events. In Fig. 8.b we present the calculated  $E_{\perp}^{\text{jet}}$  distributions. Within the statistics of the Monte Carlo runs we do not find differences between the distributions corresponding to the JJ and JgJ events.

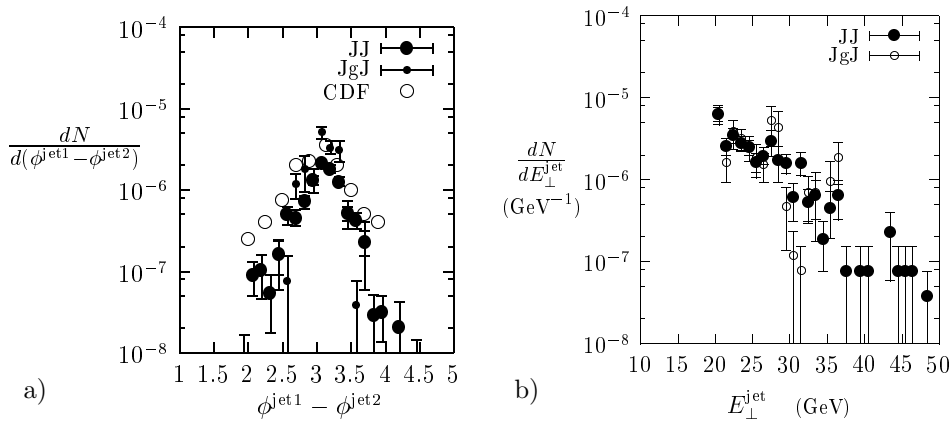


FIG. 8. (a) The  $\phi^{\text{jet1}} - \phi^{\text{jet2}}$  distributions corresponding to the CDF trigger [15]. (b) The  $E_{\perp}^{\text{jet}}$  distributions corresponding to the CDF trigger.

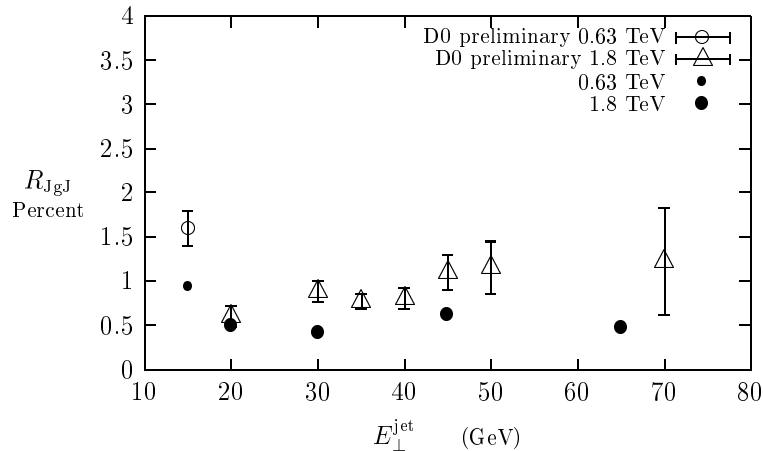


FIG. 9. The change of  $R_{\text{JgJ}}$  with the  $E_{\perp}^{\text{jet}}$ , Preliminary data from the D0 Collaboration [68] are compared to the PHOJET results obtained with SCR.

The change of  $R_{\text{JgJ}}$  with the  $E_{\perp}^{\text{jet}}$  was studied by the D0 Collaboration [68]. A modest rise of the color singlet fraction with  $E_{\perp}^{\text{jet}}$  was found. In Fig. 9 we compare the PHOJET results on  $R_{\text{JgJ}}$  with these preliminary data. The

PHOJET predictions exhibit a flat  $E_{\perp}^{\text{jet}}$  dependence being still compatible with the data <sup>2</sup>. The D0 Collaboration [68] also found  $R_{\text{JgJ}}$  at  $\sqrt{s} = 630$  GeV to be a factor  $2.6 \pm 0.6$  larger than at  $\sqrt{s} = 1.8$  TeV. The ratio of  $R_{\text{JgJ}}$  at these energies calculated with PHOJET is consistent with the data, see Fig. 9.

## IX. CONCLUSIONS AND SUMMARY

The processes implemented in PHOJET allow to study hard and soft diffraction (e.g.  $P$ - $p$ ,  $P$ - $\gamma$  and  $P$ - $P$  collisions) in many channels. We hope that this tool and forthcoming data on hard and soft single diffraction dissociation and central diffraction from TEVATRON and HERA help to answer important questions like: (i) Is soft color reconnection the correct mechanism to describe color singlet exchange processes between jets? Could this mechanism be responsible for other features of diffractive processes as well? (ii) Can hard diffraction consistently be described by pomeron structure functions? What is the low- $x$  behaviour of the pomeron structure function? (iii) Are there multiple soft and multiple hard collisions in diffraction like in  $p$ - $p$ ,  $p$ - $\gamma$  or  $\gamma$ - $\gamma$  interactions? (vi) Does a super-hard component of the pomeron exist (e.g. can the data interpreted with a direct pomeron-quark coupling)?

Single-inclusive jet pseudorapidity distributions show only a small sensitivity to a possible super-hard structure of the pomeron (see Fig. 3.b). By contrast it is possible to use the jet transverse momentum distribution to explore a super-hard pomeron structure. Furthermore, in the model, diffractive events containing jets produced by direct pomeron-parton scattering exhibit much less soft hadronic background than other JJg events. This soft underlying event feature might allow for a crucial test of the models on a super-hard pomeron. However, without using pomeron PDFs tuned to the latest HERA data reliable predictions for TEVATRON energies cannot be obtained.

All features of the JgJ events observed at TEVATRON so far are qualitatively well described in the Monte Carlo implementation of the SCR model [20]. However, first comparisons with data indicate that the ratio JgJ/JJ obtained with a simple SCR model is too small. Further investigations, higher statistics in the Monte Carlo events and more precise data are required to draw definite conclusions.

### Acknowledgments

The authors are grateful to S. Roesler for many discussions. One author (R.E.) thanks T.K. Gaisser for helpful comments and remarks. The work of R.E. is supported by the U.S. Department of Energy under Grant DE-FG02-91ER40626.

- 
- [1] V. N. Gribov, Sov. Phys. JETP **26**, 414 (1968).
  - [2] V. N. Gribov and A. A. Migdal, Sov. J. Nucl. Phys. **8**, 583 (1969).
  - [3] V. A. Abramovski, V. N. Gribov, and O. V. Kancheli, Sov. J. Nucl. Phys. **18**, 308 (1974).
  - [4] V. Innocente, A. Capella, and J. Trân Thanh Vân, Phys. Lett. **B213**, 81 (1988).
  - [5] K. Hahn and J. Ranft, Phys. Rev. **D41**, 1463 (1990).
  - [6] P. Aurenche *et al.*, Phys. Rev. **D45**, 92 (1992).
  - [7] A. Capella, U. Sukhatme, C. I. Tan, and J. Trân Thanh Vân, Phys. Rep. **236**, 225 (1994).
  - [8] A. B. Kaidalov, Phys. Rep. **50**, 157 (1979).
  - [9] A. B. Kaidalov and K. A. Ter-Martirosyan, Nucl. Phys. **B75**, 471 (1974).
  - [10] K. Goulianos, Phys. Rep. **101**, 169 (1983).
  - [11] D. Bernard *et al.*, Phys. Lett. **B166**, 459 (1986).
  - [12] P. Aurenche, F. W. Bopp, and J. Ranft, Z. Phys. **C23**, 67 (1984).
  - [13] T. Sjöstrand and M. v. Zijl, Phys. Rev. **D36**, 2019 (1987).
  - [14] S. Abachi *et al.*, Phys. Rev. Lett. **76**, 734 (1996).
  - [15] F. Abe *et al.*, Phys. Rev. Lett. **80**, 1156 (1998).
  - [16] W. Buchmüller, Phys. Lett. **B353**, 335 (1995).
  - [17] W. Buchmüller and A. Hebecker, Phys. Lett. **B355**, 573 (1995).
  - [18] A. Edin, G. Ingelman, and J. Rathsmann, Phys. Lett. **B366**, 371 (1995).
  - [19] J. F. Amundson, O. J. P. Eboli, E. M. Gregores, and F. Halzen, Phys. Lett. **B372**, 127 (1996).

---

<sup>2</sup>Very recent data of the CDF Collaboration [15] on a similar ratio show also a flat  $E_{\perp}^{\text{jet}}$  dependence

- [20] O. J. P. Eboli, E. M. Gregores, and F. Halzen, (hep-ph/9708283) (unpublished).
- [21] A. H. Mueller and W. K. Tang, Phys. Lett. **B284**, 123 (1992).
- [22] V. Del Duca and W. K. Tang, Phys. Lett. **B312**, 225 (1993).
- [23] R. Engel, Z. Phys. **C66**, 203 (1995).
- [24] R. Engel and J. Ranft, Phys. Rev. **D54**, 4244 (1996).
- [25] F. W. Bopp, R. Engel, D. Pertermann, and J. Ranft, Phys. Rev. **D49**, 3236 (1994).
- [26] B. L. Combridge, J. Kripfganz, and J. Ranft, Phys. Lett. **B70**, 234 (1977).
- [27] D. W. Duke and J. F. Owens, Phys. Rev. **D26**, 1600 (1982).
- [28] R. Engel, M. A. Braun, C. Pajares, and J. Ranft, Z. Phys. **C74**, 687 (1997).
- [29] J. L. Cardy, Nucl. Phys. **B75**, 413 (1974).
- [30] A. B. Kaidalov, L. A. Ponomarev, and K. A. Ter-Martirosyan, Sov. J. Nucl. Phys. **44**, 468 (1986).
- [31] A. Capella, A. Kaidalov, C. Merino, and J. Trân Thanh Vân, Phys. Lett. **B343**, 403 (1995).
- [32] A. Capella *et al.*, Phys. Rev. **D53**, 2309 (1996).
- [33] J. Collins, L. Frankfurt, and M. Strikman, Phys. Lett. **B307**, 161 (1993).
- [34] J. C. Collins *et al.*, Phys. Rev. **D51**, 3182 (1995).
- [35] B. Kniehl, H.-G. Kohrs, and G. Kramer, Z. Phys. **C65**, 657 (1995).
- [36] R. Engel and J. Ranft, to appear in Proceedings of The Int. Symposium on Near Beam Physics, Fermilab, Sept. 22-24, 1997 (unpublished).
- [37] G. Ingelman, presented at this meeting (unpublished).
- [38] J. D. Bjorken, Phys. Rev. **D47**, 101 (1993).
- [39] F. W. Bopp, R. Engel, J. Ranft, and A. Rostovtsev, to appear in Proceedings of the International Symposium on Photon Interactions and Photon Structure (PHOTON '97), Egmond aan Zee, The Netherlands (unpublished).
- [40] R. Engel, F. W. Bopp, D. Pertermann, and J. Ranft, Phys. Rev. **D46**, 5192 (1992).
- [41] J. W. Chapman *et al.*, Phys. Rev. Lett. **32**, 257 (1974).
- [42] J. Schamberger *et al.*, Phys. Rev. Lett. **34**, 1121 (1975).
- [43] M. G. Albrow *et al.*, Nucl. Phys. **B108**, 1 (1976).
- [44] J. C. M. Armitage *et al.*, Nucl. Phys. **B194**, 365 (1982).
- [45] R. E. Ansorge *et al.*, Z. Phys. **C33**, 175 (1986).
- [46] D. Robinson and C. E. Wulz, report UA1-TN / 89-10 (unpublished).
- [47] N. A. Amos *et al.*, Phys. Lett. **B243**, 158 (1990).
- [48] N. A. Amos *et al.*, Phys. Lett. **B301**, 313 (1993).
- [49] F. Abe *et al.*, Phys. Rev. **D50**, 5535 (1994).
- [50] K. Goulianos, Phys. Lett. **B358**, 379 (1995).
- [51] A. Capella, J. Kaplan, and J. Trân Thanh Vân, Nucl. Phys. **B105**, 333 (1976).
- [52] E. Gotsman, E. M. Levin, and U. Maor, Phys. Lett. **B353**, 526 (1995).
- [53] R. Engel, Ph.D. thesis, Universität Siegen, 1997.
- [54] K. H. Streng, Phys. Lett. **166B**, 443 (1986).
- [55] R. Engel, J. Ranft, and S. Roesler, Phys. Rev. **D52**, 1459 (1995).
- [56] M. Bozzo *et al.*, Phys. Lett. **B147**, 392 (1984).
- [57] D. Bernard *et al.*, Phys. Lett. **B186**, 227 (1987).
- [58] J. Ranft, Z. Phys. **C33**, 517 (1987).
- [59] S. Roesler, R. Engel, and J. Ranft, Z. Phys. **C59**, 481 (1993).
- [60] A. Brandt *et al.*, Phys. Lett. **B297**, 417 (1992).
- [61] T. Ahmed *et al.*, Nucl. Phys. **B435**, 3 (1995).
- [62] S. Aid *et al.*, Z. Phys. **C69**, 27 (1995).
- [63] M. Derrick *et al.*, Phys. Lett. **B346**, 399 (1995).
- [64] M. Derrick *et al.*, Phys. Lett. **B356**, 129 (1995).
- [65] M. Derrick *et al.*, Z. Phys. **C67**, 227 (1995).
- [66] M. Albrow, Fermilab–Conf–97/362 (unpublished).
- [67] F. Abe *et al.*, Phys. Rev. Lett. **79**, 2636 (1997).
- [68] B. Abbott *et al.*, Fermilab–Conf–97/250–E (unpublished).